THE JOURNAL OF BIOLOGICAL CHEMISTRY
Vol. 278, No. 31, Issue of August 1, pp. 29016–29023, 2003

Printed in U.S.A.

Structural $(\beta\alpha)_8$ TIM Barrel Model of 3-Hydroxy-3-methylglutaryl-Coenzyme A Lyase*

Received for publication, April 23, 2003, and in revised form, May 13, 2003
Published, JBC Papers in Press, May 13, 2003, DOI 10.1074/jbc.M304276200

Núria Casals,[a] Paulino Gómez-Puertas,[b] Juan Pié,[c] Cecilia Mir,[a,d] Ramón Roca,[e] Beatriz Puisac,[c,f] Rosa Aledo,[a] Josep Clotet,[a] Sebastián Menao,[c] Dolors Serra,[g] Guillermina Asins,[g] Jacqueline Till,[h] Alun C. Elias-Jones,[i] Juan C. Cresto,[j] Nestor A. Chamoles,[j] José E. Abdenur,[j] Ertan Mayatepek,[k,l] Guy Besley,[h] Alfonso Valencia,[e] and Fausto G. Hegardt[g,m]

From the [a]Unit of Biochemistry and Molecular Biology, International University of Catalonia, 08190 Sant Cugat del Vallés, [b]Bioinformatics Laboratory (CAB-CSIC), 28850 Torrejón de Ardoz, Madrid, [c]Department of Pharmacology and Physiology, University of Zaragoza, 50009 Zaragoza, [e]Protein Design Group (CNB-CSIC), Cantoblanco, 28049 Madrid, the [g]Department of Biochemistry and Molecular Biology, School of Pharmacy, University of Barcelona, Barcelona, Spain, [h]Willink Biochemical Genetic Unit, Manchester M27 4HA, United Kingdom, the [i]Department of Pediatrics, Leicester General Hospital, Leicester LE5 4PW, United Kingdom, [j]Fundación para el Estudio de las Enfermedades Neurometabólicas, 1425 Buenos Aires, Argentina, and [k]Division of Metabolic and Endocrine Diseases, University Children's Hospital, D-69120 Heidelberg, Germany

This study describes three novel homozygous missense mutations (S75R, S201Y, and D204N) in the 3-hydroxy-3-methylglutaryl-CoA (HMG-CoA) lyase gene, which caused 3-hydroxy-3-methylglutaric aciduria in patients from Germany, England, and Argentina. Expression studies in *Escherichia coli* show that S75R and S201Y substitutions completely abolished the HMG-CoA lyase activity, whereas D204N reduced catalytic efficiency to 6.6% of the wild type. We also propose a three-dimensional model for human HMG-CoA lyase containing a $(\beta\alpha)_8$ (TIM) barrel structure. The model is supported by the similarity with analogous TIM barrel structures of functionally related proteins, by the localization of catalytic amino acids at the active site, and by the coincidence between the shape of the substrate (HMG-CoA) and the predicted inner cavity. The three novel mutations explain the lack of HMG-CoA lyase activity on the basis of the proposed structure: in S75R and S201Y because the new amino acid residues occlude the substrate cavity, and in D204N because the mutation alters the electrochemical environment of the active site. We also report the localization of all missense mutations reported to date and show that these mutations are located in the β-sheets around the substrate cavity.

3-Hydroxy-3-methylglutaric aciduria (MIM246450) is a rare autosomal recessive metabolic disorder appearing in the 1st year of life. Acute episodes include vomiting, lethargy, hypotonia, and apnea, sometimes evolving to coma (1, 2). Laboratory tests reveal metabolic acidosis with severe hypoketotic hypoglycemia on fasting or during acute illness, hyperammonemia, and abnormal liver function tests. The disease is fatal in about 20% of cases (3) although the symptoms are milder after childhood. Preliminary diagnosis is based on the excretory pattern of organic acids in urine, which include 3-hydroxy-3-methylglutaric, 3-hydroxyisovaleric, 3-methylglutaconic, 3-methylglutaric, and 3-methylcrotonic acids (1, 4).

The origin of the disease is a mutation in the gene coding for 3-hydroxy-3-methylglutaryl-coenzyme A (HMG-CoA)[1] lyase (HL), which cleaves HMG-CoA to form acetyl-CoA and acetoacetate. This is the final step in the ketogenic pathway and leucine catabolism. The gene was assigned to the distal short arm of human chromosome 1p36.1 (5). It contains 9 exons and is transcribed in an mRNA of 1.7 kb (6). The presence of the protein inside mitochondria and peroxisomes has been reported. The active site of HL has been shown to include the residues Cys^{266} and His^{233} (7, 8). To date, 38 probands have been diagnosed at the molecular level, and 22 different mutations of the HL gene have been reported (5, 6, 9–19). Only one of the missense mutations described, H233R, directly affects the catalytic residues. In contrast, there is no explanation for the effect of the other five reported missense mutations in the functional structure of the enzyme.

Here we report three novel homozygous missense mutations affecting patients from Germany, England, and Argentina, and we describe the effect of these mutations in the protein activity by expression studies in *Escherichia coli*. We also propose a three-dimensional model for the human HMG-CoA lyase containing a $(\beta\alpha)_8$ barrel structure, usually called TIM barrel, predicted by the relationship between *HMGL-like* and *hisA* (1qo2) family proteins. All the missense mutations reported to date are located in the proposed structural model around the catalytic cavity, and their possible effects on enzyme activity are discussed.

MATERIALS AND METHODS

Case Reports—Patient D. S. was a 5-month-old Argentinean female born of healthy 1st cousin parents after a normal pregnancy and delivery. On physical examination, the patient had all the clinical features of

* This work was supported in part by Grant PB95-0012 from the Dirección General de Investigación Científica y Técnica, the Fundació de la Marató de TV3 (Barcelona), Grant G03/054 from the Spanish Ministry of Health, Grant 2001SGR0123 from the Generalitat de Catalunya, Spain (to F. G. H.), Grant CICYT 2002-2003 (to A. V.), a grant from the Ramon Areces Foundation (to P. G.-P.), and Grant P100/99-BM from the Diputación General de Aragón (to J. P.). The costs of publication of this article were defrayed in part by the payment of page charges. This article must therefore be hereby marked "*advertisement*" in accordance with 18 U.S.C. Section 1734 solely to indicate this fact.

[d] Recipient of a fellowship from the Universitat Internacional de Catalunya.
[f] Recipient of fellowship from the Diputación General de Aragón.
[l] Present address: Dept. of General Pediatrics, University Children's Hospital, Heinrich-Heine-University Düsseldorf, Moorenstrasse 5, D-40225 Düsseldorf, Germany.
[m] To whom correspondence should be addressed: Dept. of Biochemistry, School of Pharmacy, Avda. Diagonal 643, E-08028 Barcelona, Spain. Tel.: 34-93-402-4523; Fax: 34-93-402-4520; E-mail: hegardt@farmacia.far.ub.es.

[1] The abbreviations used are: HMG-CoA, 3-hydroxy-3-methylglutaryl-CoA; HL, HMG-CoA lyase; PDB, Protein Data Bank.

classical HMG-CoA lyase deficiency. The organic acids and acylcarnitine (3-hydroxyisovalerylcarnitine (2.42 mM) and methylglutarylcarnitine (0.09 mM)) found in blood and urine supported the diagnosis. She was given intravenous glucose and she recovered rapidly.

The first symptoms of the English proband (B. P.) appeared at 48 h of age, and tests revealed metabolic acidosis (high pyruvate and lactate), hypoglycemia (1.2 mM), and 13.9 mM bicarbonate. The organic acids (3-hydroxyisovalerate, 3-methylglutarate, 3-methylglutaconate, glutarate, adipate, and other dicarboxylic acids) found in blood and urine supported the diagnosis of 3-hydroxymethylglutaric aciduria. HMG-CoA lyase activity was 0.

Aciduria in the German patient (T. J.) first appeared at 4 months of age after DPT/HiB/polio immunization, with recurrent vomiting, muscular hypotonia, and comatose attacks. He showed hyperammonemia, liver dysfunction, and massive excretion of organic acids typical of HMG-CoA lyase deficiency. Enzyme activity was 0.2 $nmol \cdot min^{-1} \cdot mg^{-1}$ protein. The boy recovered well with intravenous glucose and at 8 years shows no mental retardation nor renal, hepatic, or cardiac abnormalities.

Fibroblast Culture and DNA Isolation—A skin biopsy was taken from the patient B. P. Fibroblast explants were cultured in 25-cm^2 flasks in Dulbecco's modified Eagle's medium, 100 IU/ml penicillin, and 100 mg/ml streptomycin, 2 mM glutamine, 10% fetal calf serum, and 95% air, 5% CO_2. Mutational analysis was performed in DNA isolated from leukocytes (D. S. and T. J.) or cultured fibroblasts (B. P.). DNA was isolated using the DNAzol® Reagent kit from Invitrogen.

PCR Amplification of Genomic DNA—To amplify all exons, 200 ng of genomic DNA was amplified in a 100-μl mixture containing 0.2 mM of each dNTP, 25 pmol of each primer, 2.5 units of *Taq* DNA polymerase in 1× PCR buffer, and 2 mM $MgCl_2$ and the primers flanking intron sequences (11). The conditions used are as follows: 98 °C for 5 min and subsequently 94 °C for 30 s, 58 °C for 30 s, 72 °C for 30 s for 35 cycles, and finally 7 min at 72 °C.

Missense Mutation Restriction Analysis—Two specific primers, mut201 and mut204, were designed to introduce an individual nucleotide mutation, which would generate a new restriction site *Nco*I or *Dra*II, respectively, in the control DNA. The mutations S201Y (c602C>A) and D204N (c610G>A) abolished the restriction sites introduced by the primers mut201 and mut204, respectively. The mutation S75R (c225C>G) abolished an *Alu*I site, present in the control DNA. Primers used in the amplifications are shown as follows. The modified nucleotide is underlined. For the Mut201 sequence primer, 5′-GGGGTGCCCACACCAATGGTGTCCCCCATG-3′; for the Mut204 sequence primer, 5′-TGATCCCTGGGGTGCCCACACCAATGGGG-3′; and for the I3R1 sequence primer, 5′-CCTATGTTCTCAACTTCTAC-3′.

Genomic fragments amplified with primers F7E (18) and Mut201, with primers F7E and Mut204, or with primers F1 (15) and I3R1 in controls and patients were used as substrates for analytical digestion with *Nco*I, *Dra*II, or *Alu*I, respectively. Five units of restriction enzymes were added to 20 μl of reaction medium. Digestions were incubated for 3 h at 37 °C; the resulting restriction fragments were fractionated on a 4.5% metaphor-agarose gel.

Construction of Expression Plasmids—HMG-CoA lyase cDNA was amplified by reverse transcriptase-PCR from 1 μg of total RNA isolated from control human fibroblasts, using Superscript II kit (Amersham Biosciences), as described by the manufacturer. The region of the cDNA coding for the mature protein plus 5′ Met and Gly codons was amplified with *Pfu* DNA polymerase (Stratagene) and primers that introduced an *Nco*I site (5′-GCACCTCATCCATGGGCACT-3′) and a *Bam*HI site (5′-CCCCAGGGATCCAGGTGGGC-3′) at the ends of the amplified fragment. The 950-bp PCR fragment was cloned into *Nco*I/*Bam*HI-cut pTrc99A plasmid to give the expression plasmid pTr-HLwt. The insert was sequenced with Applied Biosystems 373 automated DNA sequencer to verify that no mutations had been introduced during PCR amplification.

Mutants S75R, S201Y, and D204N of HL were constructed using the "Quick Change" PCR-based mutagenesis procedure (Stratagene) with the pTr-HL-wt plasmid as a template. Primer 5′-TATAGAAACCACCAGGTTTGTGTCTCCTAAG-3′ was used to construct pTr-HL-75R; primer 5′-GCTGCTACGAGATCTACCTGGGGGACACCATTG-3′ was used to construct pTr-HL-201Y; and primer 5′-GAGATCTCCCTGGGGAACACCATTGGTGTGG-3′ was used to construct pTr-HL-204N. The appropriate substitutions and the absence of unwanted mutations were confirmed by sequencing the inserts.

Expression of HL in E. coli—*E. coli* JM105 cells transformed with the expression plasmids were grown in LB broth supplemented with ampicillin (50 μg/ml) at 25 °C. When A_{600} = 0.6, the expression of HL was induced by addition of isopropyl-1-thio-β-D-galactopyranoside to a final concentration of 1 mM. After 6 h of induction, cells were recovered by centrifugation at 5,000 × *g* for 15 min at 4 °C and frozen to −70 °C until required for use.

Cell pellets were resuspended in lysis buffer (NaCl 50 mM, Tris-HCl, pH 7.5, 5 mM, DNase 10 μg/ml, RNase 10 μg/ml, phenylmethylsulfonyl fluoride 0.6 mM, pepstatin 1 μg/ml, leupeptin 2 μg/ml, lysozyme 1 mg/ml) and incubated for 15 min at 4 °C. Afterward, the tubes were frozen to −70 °C and thawed to 37 °C. Soluble proteins were recovered by centrifugation at 10,000 × *g* for 10 min at 4 °C and immediately frozen and stored at −70 °C. Protein quantification was performed using the Bio-Rad protein assay with bovine albumin as standard.

HMG-CoA Lyase Activity—HMG-CoA lyase activity was measured by simple spectrophotometric method that determines the amount of acetoacetate produced (20). For HL-specific activity determination, 2 μg of soluble protein extracts and 800 nmol of substrate (HMG-CoA) were used. In the case of mutation extracts, determinations were also carried out with 20 or 75 μg of soluble protein extract. The reaction assay was performed at 37 °C for 15 min in a final volume of 250 μl. One enzyme unit represents the formation of 1 μmol of acetoacetate in 1 min. For K_m determinations, 2 μg of soluble crude extract was used. HMG-CoA concentrations ranged from 400 to 6400 μM. Results are given as mean values of at least four independent experiments.

Western Blot Analyses—A polyclonal rabbit antibody against residues 307–321 of human HL (which recognizes the COOH terminus of the enzyme) was raised by Sigma-Genosys. 50 μg of *E. coli* protein extract was subjected to SDS-PAGE. Electroblotting to nitrocellulose sheets was carried out for 2 h at 120 mA. Immunodetection of HL was performed using the antibody anti-HL (dilution 1:10,000), and the blots were developed with the ECL Western blotting system from Amersham Biosciences.

Prediction of a Structural Model for HMGL_HUMAN—The multiple sequence alignment used to provide the anchor points of the modeled human 3-hydroxy-3-methylglutaryl-CoA lyase (HMGL_HUMAN) to the template three-dimensional structure 1qo2 (*hisA* (21)) was prepared by aligning the *HMGL_like*-PF00682- and *His_biosynth*-PF00977-Pfam data base families (22). This alignment is similar to that obtained elsewhere (23) after four interactions of a PSI-Blast search of the NR protein sequence data base from the NCBI, using the amino acid sequence of 1qo2 as seed (24).

To obtain a three-dimensional model of HMGL_HUMAN (amino acids 36–287), the program Swiss-Pdb Viewer and the SWISS-MODEL server facilities (25–28) (www.expasy.ch/swissmod/SWISS-MODEL.html) were used. The atomic coordinates of the $(\beta\alpha)_8$ barrel template structure used to model the protein were obtained from the Protein Data Bank (PDB) (www.rcsb.org/pdb; entry 1qo2). The atomic coordinates of the 3-hydroxy-3-methylglutaryl-CoA molecule were obtained from the PDB entry 1qax. All missense mutants described in the study were modeled using the HMGL_HUMAN model as template.

The quality of the HMGL_HUMAN model was checked using the programs ProsaII (Center of Applied Molecular Engineering, Salzburg, Austria (29); the WHAT-CHECK routines (30) from the WHAT IF program (31) and the PROCHECK validation program from the SWISS-MODEL server facilities (32). The comparison of the values from the template structure 1qo2 *versus* the proposed HMGL_HUMAN model is accessible through the URL, www.cnb.uam.es/~pagomez/HM_Check.html. Briefly, the overall quality values of the model are poorer than the usual ones for experimental x-ray or NMR structures but are acceptable in the expected region for protein structure models.

The interaction between HMG-CoA as the substrate and the proposed model was calculated using the macromolecular docking program "Hex" (33) based on spherical polar Fourier correlations. The picture of the surface, section, and electrostatic potentials for the proposed protein models was produced using the GRASP program (34), and the ribbon plots were drawn with RASMOL (35).

RESULTS

Localization of the Mutations Responsible for 3-Hydroxy-3-methylglutaric Aciduria—DNA extracted from lymphocytes from either patients (D. S. and T. J.) or fibroblast cultures obtained from skin biopsies (B. P.) were used as templates for amplification by PCR of the nine exons of HMG-CoA lyase using primers described previously (11). The size of the amplified fragments from the patients was identical to control. This suggested that point mutations in the HMG-CoA lyase gene were responsible for the disease. Sequencing of the amplified exons showed that patient T. J. had the new homozygous mu-

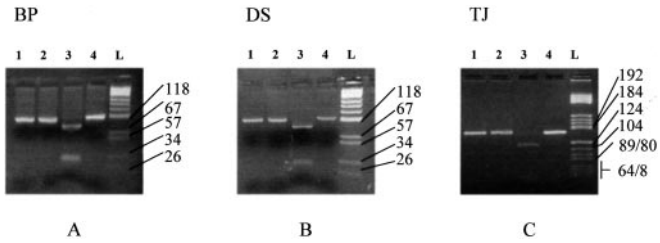

FIG. 1. **Restriction enzyme analysis of mutations S75R, S201Y, and D204N.** *A*, patient B. P, and control genomic DNA-amplified fragments using F8/Mut201 primers were incubated with *Nco*I. Two fragments of 88 and 30 bp (*lane 3*) in the control and only one fragment of 115 bp (*lane 4*) in the patient are observed. *Lanes 1* and *2* are amplified fragments of control and patient without digestion. *B*, patient D. S. and control genomic DNA-amplified fragments using F8/Mut204 primers were incubated with *Dra*II. Two fragments of 90 and 30 bp in the control DNA (*lane 3*) and only one fragment of 120 bp (*lane 4*) in the patient are observed. *Lanes 1* and *2* are amplified fragments of control and patient without digestion. *C*, patient T. J. and control genomic DNA-amplified fragments using F1/I3R1 primers were incubated with *Alu*I. Two fragments of 117 and 47 bp in the control (*lane 3*) and only one fragment of 164 bp in the patient (*lane 4*) are observed. *Lanes 1* and *2* are amplified fragments of control and patient without digestion. *Lane L* is molecular weight marker.

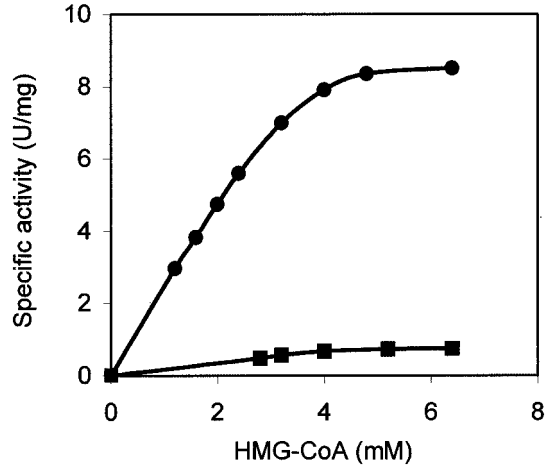

FIG. 2. **Saturation kinetics of wild type and D204N mutant HL expressed in *E. coli*.** 2 μg of crude extracts from *E. coli* expressing wild type (*circles*) or D204N HL (*squares*) protein were assayed for HL activity with different concentrations of HMG-CoA.

tation S75R (c225C>G), patient B. P. had the new homozygous mutation S201Y (c602C>A), and patient D. S. had the new homozygous mutation D204N (c610G>A). The mutations localized by sequencing were corroborated by restriction analysis of PCR-amplified fragments (Fig. 1).

Residues affected by mutation presented a high degree of conservation compared with HL from other species. Asp[204] is invariant in the various HMG-CoA lyases from mammals (human, bovine, rat, and mouse), chicken, plants (*Arabidopsis thaliana*, and rice), and bacteria (*Pseudomonas mevalonii*, *Bacillus subtillis*, and *Rhodospirillum rubrum*) for which primary structures have been elucidated. Moreover, Asp[204] is also invariant in 59 enzymes whose mechanism of reaction is analogous to HMG-CoA lyase, such as homocitrate synthase, 2-isopropylmalate synthase, oxovalerate aldolase, and pyruvate carboxylase from mammals, yeast, bacteria, and Archaea. Ser[201] is conserved in the HMG-CoA lyases of all organisms reported as well as Ser[75], which is conserved in all HMG-CoA lyases save those of *R. rubrum* and *P. mevalonii,* in which it is replaced by an alanine.

Expression of Mutant Proteins in E. coli and Determination of Enzymatic Activity—The expression system used to overexpress mature wild type and mutated HMG-CoA lyase was that described by Roberts *et al.* (36). *E. coli* JM105 cells were transformed with pTr-HL-wt, pTr-HL-75R, pTr-HL-201Y, and pTr-HL-204N plasmids or the empty vector (pTr-0), and three different cell clones for each plasmid construct were induced to express HL. Expression levels were the same in the three clones of each construct, and no expression was detected by Western blot in cells transfected with the empty vector (data not shown).

Specific HMG-CoA lyase activity from wild type and mutants was determined in the soluble fraction of crude extracts of transformed *E. coli*. Mutations S75R and S201Y completely abolished the enzyme activity, even when 75 μg of total protein extract was used in the assay. It was impossible to perform saturation kinetics and determine the K_m value for these mutants. The calculated V_{max} for the wild type was 9.5 units/mg protein and 1.35 units/mg for mutant D204N. The apparent K_m of the expressed protein was 3.1 mM for the wild type and 6.6 mM for the mutant D204N. Therefore, the mutant decreased V_{max} 7.1-fold and increased the K_m 2.1-fold with respect to the wild type (Fig. 2). The catalytic efficiency (V_{max}/K_m) for the mutated enzyme was 6.6% of the wild type, which confirmed the aciduria observed in the patient.

Structural Model of Human HMG-CoA Lyase—A relationship was found previously between the 3-hydroxy-3-methylglutaryl-CoA lyase (*HMGL)-like* family of proteins (22) and the TIM-barrel *hisA* gene from *Thermotoga maritima* (Protein Data Bank entry 1qo2 (21), which suggested that a $(\beta\alpha)_8$ barrel structure (also known as TIM barrel) could be adopted by the *HMGL-like* family (23). This type of structure consists of an 8-fold repetition of a β-sheet-loop-α-helix-loop motif, with the β-sheets forming the inner face of the barrel and the α-helices the external face. In addition, using methods based on recursive intermediate sequence searching (37) as well as the hierarchical classification of proteins contained in the PROTOMAP data base (38), a further relationship was found between HMG-CoA lyase and the HisA (1qo2) protein families. On the basis of all these results, multiple alignment of both protein families was performed (Fig. 3), and the information extracted was used to construct a three-dimensional model of the human HMG-CoA lyase, using the structure of *T. maritima* HisA protein as a template (Fig. 4). This model is a $(\beta\alpha)_8$ barrel with short loops at the NH_2-terminal face, and long and probably non-structured loops at the COOH-terminal face. The secondary structure prediction for the eight β-sheets and α-helices of the HMG-CoA lyase sequences calculated using the PHD method (39, 40) is compatible with the alignment made using sequence searching methodologies, showing a high correlation between structural and sequence alignments.

In the proposed model for human HMG-CoA lyase the side chains of the barrel forming β-sheets conform a central cavity, which is similar to the structure of other TIM barrel-like enzymes such as methylmalonyl-CoA mutase (PDB entry 7req) (41). A section of the proposed model (Fig. 4*C*, *right panel*) shows the contour of the central cavity where the calculations from the macromolecular docking program "Hex" localized the substrate, suggesting that 3-hydroxy-3-methylglutaryl-CoA crosses the cavity and locates the small 3-hydroxy-3-methylglutaryl head close to the His[233]-defined active site. The location of the active enzyme locus in the COOH-terminal face of the β-barrel is consistent with the general disposition of the active sites in the TIM barrel-like structures (42).

Once the three-dimensional model for human HL was established, residues affected by the three novel mutations described here (Ser[75], Ser[201], and Asp[204]) and by all missense mutations reported previously (Arg[41], Asp[42], Val[70], His[233], Leu[263], and Glu[279]) (8, 9, 10, 13, 18) were localized in the model. Interest-

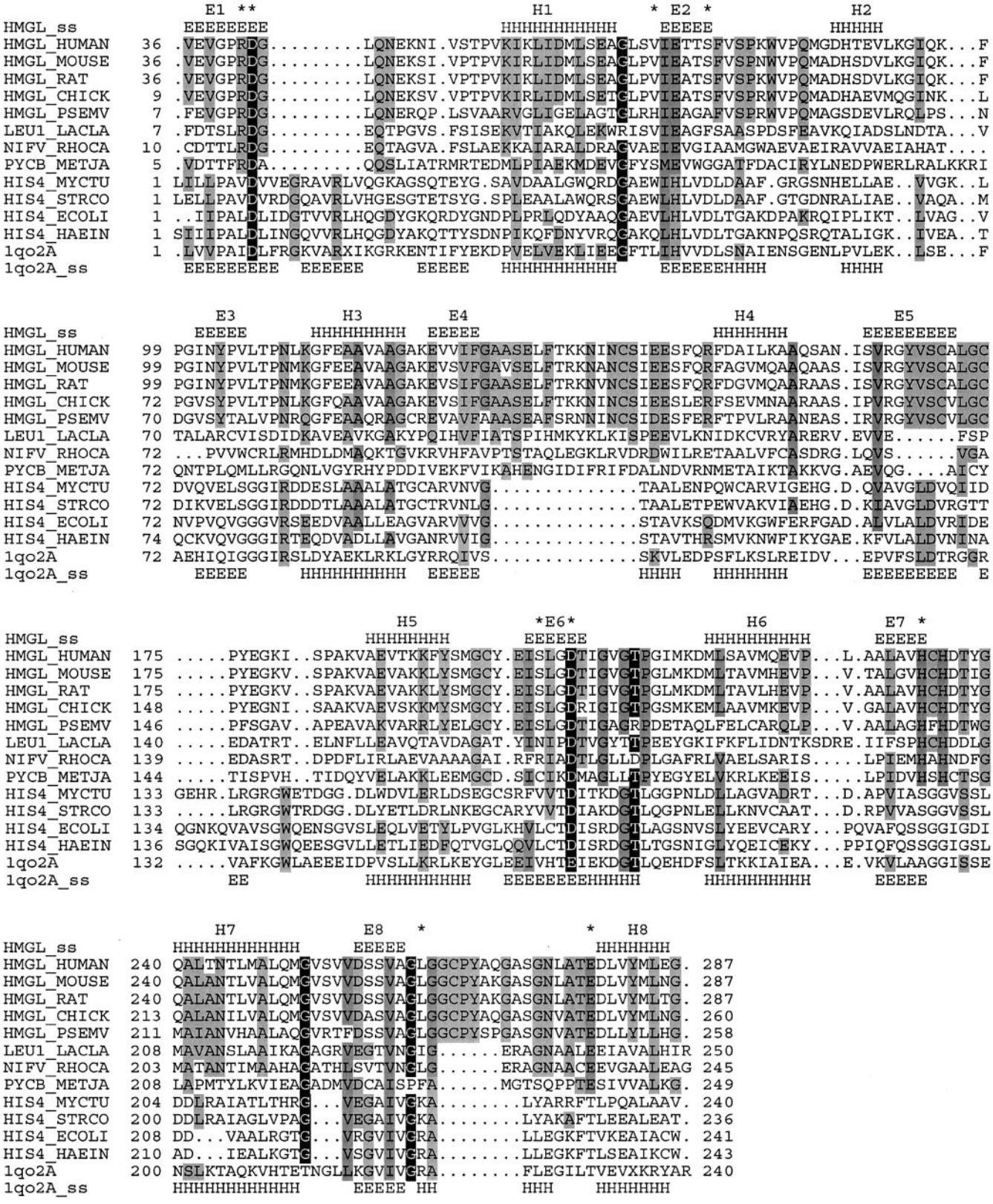

FIG. 3. **Multiple sequence alignment of representative proteins of the *HMGL_like* and *His_biosynth* families.** The amino acid sequence and the secondary structure of the PDB structure 1qo2A included in the alignment were both derived from the FSSP data base (48). The protein family definition corresponds to the Pfam data base (22). The location of the β-strands and α-helices of the central 8-fold ($\beta\alpha$) barrel of the proposed model for HMGL_HUMAN are indicated (*E*, β-strand; *H*, α-helix) and numbered from 1 to 8. The positions of the HMGL_HUMAN amino acids Arg[41], Asp[42], Val[70], Ser[75], Ser[201], Asp[204], His[233], Leu[263], and Glu[279] are marked with *asterisks*.

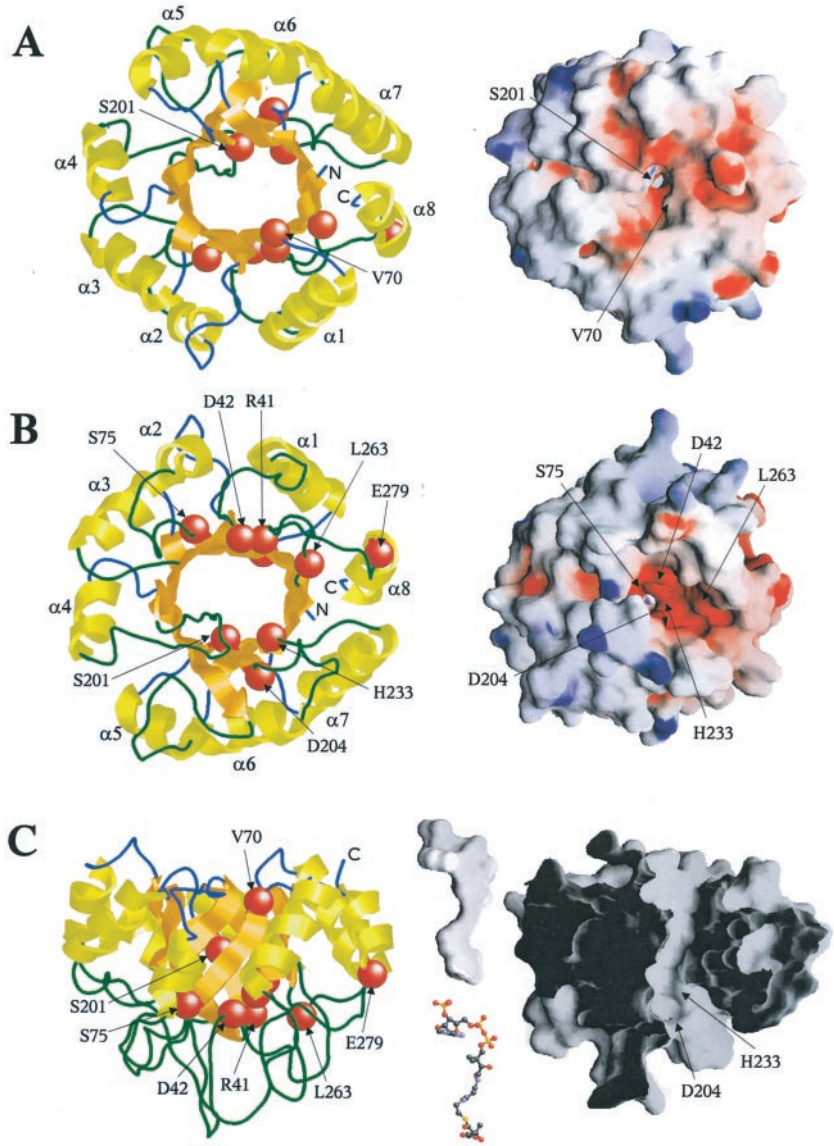

FIG. 4. **Ribbon plot and solvent-accessible surface representations of the proposed model of HMGL_HUMAN.** *A*, view from the NH_2-terminal face of the central β-barrel. *Left*, the β-strands of the central barrel are in *orange*, and the α-helices are in *yellow*, and they are numbered as in Fig. 3. The loops at the COOH- and the NH_2-terminal faces are colored in *green* and *blue*, respectively; the secondary structure elements of the loops are not shown. The positions of the NH_2 and COOH termini are indicated. The HMGL_HUMAN amino acids Arg^{41}, Asp^{42}, Val^{70}, Ser^{75}, Ser^{201}, Asp^{204}, His^{233}, Leu^{263}, and Glu^{279} are represented as *red spheres*. *Right*, the electrostatic potential (−15 (*red*) to +15 kT (*blue*)) has been plotted on to the model surface, and the approximate positions of some residues are shown. *B*, view from the COOH-terminal face of the central β-barrel; colors are as in *A*. *C*, *left*, side view of the ribbon plot representation of the model; colors are as in *A*. *Right*, slice section of the model surface representation along the putative substrate cavity. The approximate positions of the HMGL_HUMAN D204 and His^{233} residues are indicated. A solvent-accessible surface and "*ball-and-stick*" representations of 3-hydroxy-3-methylglutaryl-CoA have been included.

ingly, all the mutated residues (marked as *red spheres* in Fig. 4) except Glu^{279} are localized in the β-sheets and form part of the central cavity, where the HMG-CoA substrate is assumed to be accommodated.

When Val^{70}, Ser^{75}, and Ser^{201} are replaced by Leu^{70}, Arg^{75}, and Tyr^{201}, the proposed substrate cavity is occluded by the longer side chain of the mutated amino acids, and the entrance of the substrate is prevented (Fig. 5), which is consistent with the complete absence of activity observed in expression studies performed with mutants S75R and S201Y.

Some of the residues that can be mapped with confidence are those defined previously as essential for the enzyme activity on the basis of mutational studies. His^{233}, reported as the main amino acid responsible for HMG-CoA lyase catalysis, is located on β-sheet 7 beside the substrate cavity (Figs. 3 and 4*B*). Kinetic analysis with site-directed mutants H233R and H233A showed a decrease in activity of 4 orders of magnitude (8), without modification of the K_m. In the model, the catalytic His^{233} is located exactly at the site in which the 3-hydroxy-3-methylglutaryl group is connected with the CoA, thus validating the model. His^{235} (suggested to have an important function on cation binding) is located at 5.3 Å from His^{233}, which could explain the effect of site-directed mutants (H235A and H235D) on catalytic activity (1:15 with respect to wild type) and substrate affinity (K_m was increased 4-fold) (43).

Because Asp^{204} is close to His^{233} (less than 4 Å) in the model (Fig. 4*B*), we propose that the third novel mutation here described, D204N, could affect the activity of the enzyme by changing the polarity of the active center, which fits with the decreased V_{max} observed in the expressed protein.

In addition, Arg^{41} and Asp^{42}, which are on the first β-sheet (Fig. 3), are close to the catalytic residue His^{233} (Fig. 4). Mutations in these amino acid residues R41Q, D42H, and D42G, responsible for 3-hydroxy-3-methylglutaric aciduria in some patients (13), produce changes of charge, which may also affect the efficiency of catalysis. On the other hand, Leu^{263} located close to β-sheet 8, surrounds the cavity and is three amino acids away from Cys^{266}, which is considered to be the residue to which the acetoacetic group binds before leaving the enzyme after catalysis (7). Mutation L263P (18) may interfere with the positioning of the acetoacetic group before leaving the enzyme. Mutation E279K (9) is at the beginning of α-helix 8 (Fig. 3), and the model cannot directly explain the absence of enzyme activity in this mutated enzyme, because it is located outside the inner cavity (Fig. 4). Because some proteins that fold as TIM barrels utilize loop movements to close the active site once the substrate is bound (44), mutation E279K may block this effect in catalysis.

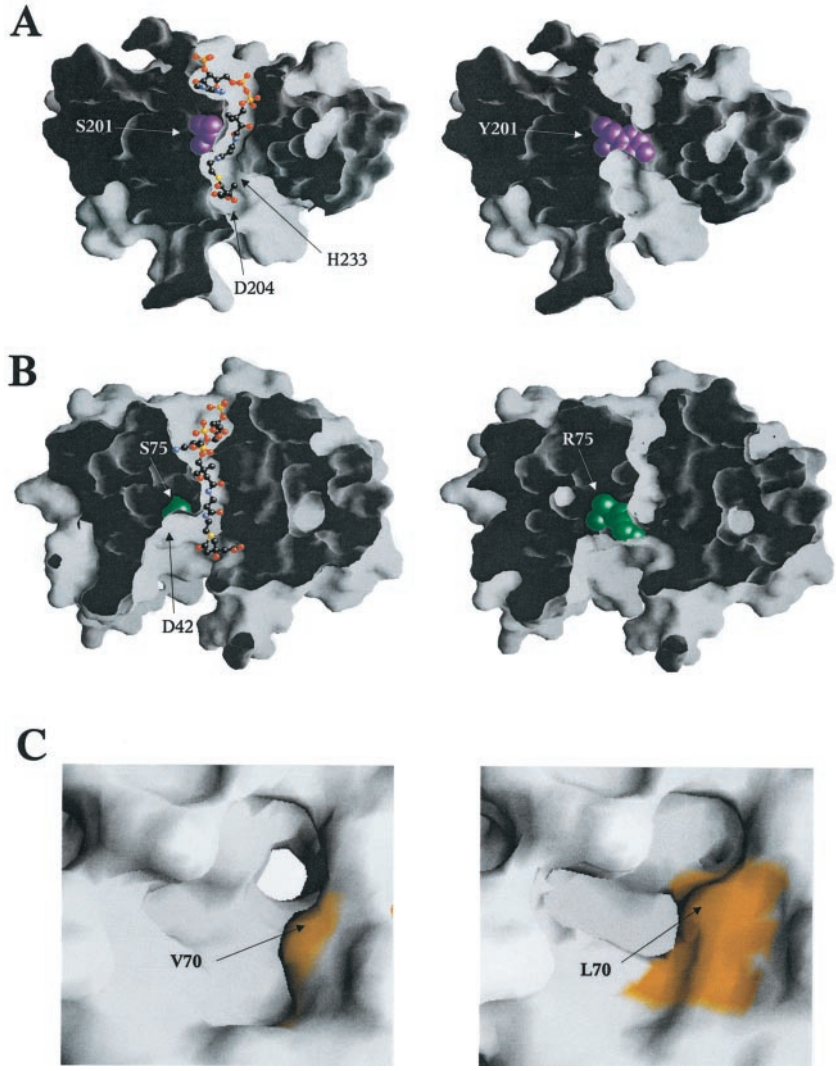

FIG. 5. *A*, $Ser^{201} \rightarrow$ Tyr mutant. *Left*, slice section of the model surface representation along the putative substrate cavity. The approximate positions of the HMGL_HUMAN Asp^{204} and His^{233} residues are indicated. The atoms of Ser^{201} are represented as *purple spheres*. A *ball-and-stick* representation of a 3-hydroxy-3-methylglutaryl-CoA molecule has been inserted into the model putative substrate cavity solely to illustrate the proposed substrate-enzyme structural interaction. *Right*, slice section of the mutant $Ser^{201} \rightarrow$ Tyr surface model showing the occlusion of the putative substrate cavity. The atoms of the Tyr^{201} amino acid are represented as *purple spheres*. *B*, $Ser^{75} \rightarrow$ Arg mutant. *Left*, slice section of the model along the putative substrate cavity. The view of this section is approximately the opposite that shown in *A*. The atoms of Ser^{75} are represented as *green spheres*. *Right*, slice section of the mutant $Ser^{75} \rightarrow$ Arg showing the location of the Arg^{75} atoms (*green spheres*) occluding the substrate cavity. *C*, $Val^{70} \rightarrow$ Leu mutant. Details of the NH_2-terminal face of the wild type protein surface model (*left*) and the $Val^{70} \rightarrow$ Leu mutant (*right*). The *orange* area occluding the end of the cavity (*right*) represents the surface of the Leu^{70} side group.

DISCUSSION

Mutational studies in patients suffering from 3-hydroxy-3-methylglutaric aciduria permit the detection of residues that are important for HL activity. The three novel mutations described here dramatically reduce the catalytic efficiency of the enzyme as demonstrated by expression studies in *E. coli*. S75R and S201Y completely abolished the enzyme activity, whereas D204N, very close to S201Y, reduced catalytic efficiency to 6.6% of the wild type. However, these studies do not indicate how these mutations produce the enzyme dysfunction. So we built a structural model of the enzyme that could explain the effect of each mutation on the enzyme structure and predict the effect of the new mutations.

Enzymes containing the $(\beta\alpha)_8$ barrel structural fold account for up to 10% of all the enzymes of the central metabolism pathways and support a wide variety of functions (42). The amino acids conforming the active locus are generally located at the COOH-terminal ends of the β-sheets and at the loops that connect the β-sheets to the α-helices (42). Copley and Bork (23), using the Psi-Blast sequence-based search method (24), provided compelling evidence that most of the known and predicted TIM barrels found in central metabolism share not only a structural fold but also a common evolutionary origin. These authors also found related sequences in enzymes of central metabolism whose three-dimensional structure has not yet been solved, although it could be TIM barrel-like folds on the basis of sequence similarity. A relation was found between members of the Pfam HMG-like (22) family of proteins and the TIM-barrel *hisA* gene from *T. maritima* (PDB entry 1qo2 (21)), leading to the suggestion that a $(\beta\alpha)_8$ barrel structure could be adopted by the HMG-like family.

Two other independent approaches supported a direct sequence relationship between the human HMG-CoA lyase and the HisA (1qo2) respective protein families. First, a program based on recursive intermediate sequence search methodology (37) confirmed a relation between those two families through a third family in the Pfam *trp_syntA* profile. In linking (or intermediate search) methods (45–48) the two proteins are considered to be related if either their similarity score is above a certain cut-off or if there is a third protein related to both above a cut-off, following a transitive principle. Further evidence of sequence relation can be found at the PROTOMAP site (www.protomap.cs.huji.ac.il), which offers a hierarchical classification of the SwissProt proteins into clusters of related proteins (38). The relation described in PROTOMAP links at a lower reliability level "1e-0" the clusters 257 (HMGL proteins and related) and 503 (HisA proteins and related) through the small cluster 2889, related in addition to the cluster 163 (trp_synt proteins and related). On the basis of these sequence relations we suggest an alignment combining the Pfam *HMGL_like* and *His_biosynth* families of proteins (Fig. 3). In turn, this alignment was used to construct a three-dimensional model of the human HMG-CoA lyase, using the structure of the *T. maritima* HisA protein (PDB entry 1qo2) as template.

The proposed structural model for HMG-CoA lyase corresponds to a $(\beta\alpha)_8$ barrel (Fig. 4) with short loops on the NH_2-terminal face and, in contrast, long and probably non-structured loops on the COOH-terminal face of the β-barrel. The model is not accurate enough to infer the precise location of all amino acids, because major movements of backbone and side chains are expected (49). However, it is sufficient to provide a suitable framework to determine the general shape, the arrangement of the structural elements, and the localization of key residues. In the case of *T. maritima* HisA protein (PDB entry 1q02), the average in root mean square deviation, as deduced from the data present in the FSSP (fold classification based on structure-structure alignment of proteins) data base, is less than 3.5 Å for TIM barrels with values of number of aligned residues and percent identity in the same range as the ones between HMG-CoA lyase and HisA protein (227 residues and 9%, respectively) (50).

Nine missense mutations producing 3-hydroxy-3-methylglutaric aciduria have been described so far in the HMG-CoA lyase gene. Some of the residues that can be mapped with confidence in the model have been defined previously as essential to the enzyme activity based on mutational studies: His[233] (8, 18), which is considered as the active site, Arg[41], and Asp[42] (13). In the present model, all these amino acids, as well as Leu[263] (18) and Asp[204] (this paper), are located on the COOH-terminal face of the barrel forming β-sheets 1, 6, 7, and 8. All surround the end of a central cavity that runs through the entire protein structure (Fig. *4C*), probably forming part of an active locus, where the head of HMG-CoA fits to be split off. The location of all these functionally essential residues in the COOH-terminal face of the β-barrel is consistent with the general arrangement of the active sites in the TIM barrel-like structures (42). Because they are all close to His[233] in the modeled structure, these mutations could affect the activity of the enzyme by changing the appropriate environmental requirements of the active center. The kinetic behavior of D204N-expressed protein is in accordance with the model; the catalytic efficiency is decreased 15.1-fold (6.6%) in respect to the wild type, whereas the substrate affinity is barely modified (the apparent K_m only doubles in D204N in respect to the wild type). The loss of enzyme activity of the mutants S75R and S201Y (this paper) and of V70L (10) has an alternative explanation within the proposed model. In the mutant proteins the side chains of the Arg[75] and of Tyr[201] are much larger than those of Ser[75] and Ser[201] (wild type) and may occlude the proposed cavity, preventing the entrance of the substrate (Fig. 5, *A* and *B*). These changes may explain the lack of enzyme activity.

These results indicated that in HL not only the amino acids that participate directly in the catalytic reaction (Cys[266] and His[233]) but probably all the amino acids surrounding the substrate cavity are critical for enzyme activity. Although Glu[279] is outside the central cavity (it is in α-helix 8), it may play a putative role in catalysis by utilizing loop movements to close the active site once the substrate is bound, as has been shown in some enzymes that fold as TIM barrels (44). This would correlate with the finding that patient having mutation E279K did not develop lethal symptoms (onset of the disease was at 7 months, residual HMG-CoA lyase activity was 2% of the wild type, and patient development at 4.4 years is normal) (9), and the involvement of Glu[279] in catalysis in this patient could be only partially impeded by the E279K substitution.

Other possible speculations on the role of specific residues previously identified as important for the enzyme activity, such as His[235] (43) or Cys[266] (7), can be based on their location in the structural model. Thus, His[235] is located at a relatively short distance from the substrate (5.3 Å), which could explain the effect of mutants H235A and H235D in both catalytic activity (1:15 with respect to wild type) and substrate affinity (K_m was increased 4-fold) (50). Cys[266], which localizes in the COOH-terminal loop between β-strand 8 and α-helix 8, could take part in enzyme function through putative loop movements, as supposed for Glu[279]. Although these structural arrangements could explain the lack of activity of the HMGL_HUMAN mutants described, these structural data should be considered with caution, as they are derived from a low resolution homology-based model.

Expression studies to identify the crystallographic structure of the HL protein are being carried out in our laboratory, in order to corroborate the model and improve the precision with which the amino acids are localized.

Acknowledgment—The editorial help of Robin Rycroft is gratefully acknowledged.

REFERENCES

1. Wysocki, S. J., and Hahnel, R. (1986) *J. Inherited Metab. Dis.* **9,** 225–233
2. Gibson, K. M., Breuer, J., Kaiser, K., Nyhan, W. L., McCoy, E. E., Ferreira, P. Greene, C. L., Blitzer, M. G., Shapira, E., Reverte, F., Conde, C., Bagnell, P., and Cole, D. E. C. (1988) *J. Inherited Metab. Dis.* **11,** 76–87
3. Sweetman, L., and William, J. C. (1995) in *The Metabolic and Molecular Basis of Inherited Disease* (Schreiver, C. R., Beaudet, A. L., Sly, W. S., and Valle, D., eds) Vol. 1, 7th Ed., pp. 1400–1402, McGraw-Hill Inc., New York
4. Faull, K. F., Bolton, P. D., Halpern, B., Hammond, J., and Danks, D. M. (1976) *Clin. Chim. Acta* **73,** 553–559
5. Wang, S. P., Nadeau, J. H., Duncan, A., Robert, M. F., Fontaine, G., Schappert, K., Johson, K. R., Zietkiewicz, E., Hruz, P., Miziorko, H., and Mitchell, G. A. (1993) *Mamm. Genome* **4,** 382–387
6. Mitchell, G. A., Robert, M. F., Hruz, P. W., Wang, S., Fontaine, G., Behnke, C. E., Mende-Mueller, L. M., Schappert, K., Lee, C., Gibson, K. M., and Miziorko, H. M. (1993) *J. Biol. Chem.* **268,** 4376–4381
7. Roberts, J. R., Narasimhan, C., and Miziorko, H. M. (1995) *J. Biol. Chem.* **270,** 17311–17316
8. Roberts, J. R., Mitchell, G. A., and Miziorko, H. (1996) *J. Biol. Chem.* **271,** 24604–24609
9. Muroi, J., Yorifuji, T., Uematsu, A., Shigematsu, Y., Onigata, K., Maruyama, H., Nobutoki, T., Kitamura, A., and Nakahata, T. (2000) *Hum. Genet.* **107,** 320–326
10. Mitchell, G. A., Robert, M. F., Fontaine, G., Wang, S., Lambert, M., Cole, D., Lee, C., Gibson, K. M., and Miziorko, H. (1992) *Am. J. Hum. Genet.* **51,** (suppl.) 173
11. Wang, S. P., Robert, M. F., Gibson, K. M., Wanders, R. J. A., and Mitchell, G. A. (1996) *Genomics* **33,** 99–104
12. Mitchell, G. A., Jakobs, C., Gibson, K. M., Robert, M. F., Burlina, A., Dionisi-Vici, C., and Dallaire, L. (1995) *Prenatal Diagn.* **15,** 725–729
13. Mitchell, G. A., Ozand, P. T., Robert, M.-F., Ashmarina, L., Roberts, J., Gibson, K. M., Wanders, R. J., Wang, S., Chevalier, I., Plöchl, E., and Miziorko, H. (1998) *Am. J. Hum. Genet.* **62,** 295–300
14. Buesa, C., Pié, J., Barceló, A., Casals, N., Mascaró, C., Casale, C. H., Haro, D., Duran, M., Smeitink, J. A. M., and Hegardt, F. G. (1996) *J. Lipid Res.* **37,** 2420–2432
15. Pié, J., Casals, N., Casale, C. H., Buesa, C., Mascaró, C., Barceló, A., Rolland, M. O., Zabot, T., Haro, D., Eyskens, F., Divry, P., and Hegardt, F. G. (1997) *Biochem. J.* **323,** 329–335
16. Casals, N., Pié, J., Casale, C. H., Zapater, N., Ribes, A., Castro-Gago, M., Rodriguez-Segade, S., Wanders, R. J. A., and Hegardt, F. G. (1997) *J. Lipid Res.* **38,** 2303–2313
17. Casale, C. H., Casals, N., Pié, J., Zapater, N., Pérez-Cerdá, C., Merinero, B., Martínez-Pardo, M., García-Peñas, J. J., García-Gonzalez, J. M., Lama, R., Poll-The, B.-T., Smeitink, J. A. M., Wanders, R. J. A., Ugarte, M., and Hegardt, F. G. (1998) *Arch. Biochem. Biophys.* **349,** 129–137
18. Zapater, N., Pié, J., Lloberas, J., Rolland, M.-O., Leroux, B., Vidailhet, M., Divry, P., Hegardt, F. G., and Casals, N. (1998) *Arch. Biochem. Biophys.* **358,** 197–203
19. Funghini, S., Pasquini, E., Cappellini, M., Donati, M. A., Morrone, A., Fonda, C., and Zammarchi, E. (2001) *Mol. Genet. Metab.* **73,** 268–275
20. Wanders, R. J. A., Schutgens, R. B. H., and Zoeters, P. H. M. (1988) *Clin. Chim. Acta* **171,** 95–101
21. Lang, D., Thoma, R., Henn-Sax, M., Sterner, R., and Wilmanns, M. (2000) *Science* **289,** 1546–1550
22. Bateman, A., Birney, B., Durbin, R., Eddy, S. R., Howe, K. L., and Sonnhammer, E. L. (2000) *Nucleic Acids Res.* **28,** 263–266
23. Copley, R. R., and Bork, P. (2000) *J. Mol. Biol.* **303,** 627–640
24. Altschul, S. F., Madden, T. L., Schäffer, A. A., Zhang, J., Zhang, Z., Miller, W., and Lipman, D. J. (1997) *Nucleic Acids Res.* **25,** 3389–3402
25. Guex, N., and Peitsch, M. C. (1997) *Electrophoresis* **18,** 2714–2723
26. Guex, N., Diemand, A., and Peitsch, M. C. (1999) *Trends Biochem. Sci.* **24,** 364–367
27. Peitsch, M. C. (1995) *Bio/Technology* **13,** 658–660
28. Peitsch, M. C. (1996) *Biochem. Soc. Trans.* **24,** 274–279
29. Sippl, M. J. (1993) *Proteins* **17,** 355–362
30. Hooft, R. W. W., Vriend, G., Sander, C., and Abola, E. E. (1996) *Nature* **381,** 272

31. Vriend, G. (1990) *J. Mol. Graphics* **8,** 52–56
32. Laskowski, R. A., MacArthur, M. W., Moss, D. S., and Thornton, J. M. (1993) *J. Appl. Crystallogr.* **26,** 283–291
33. Ritchie, D. W., and Kemp, G. J. (2000) *Proteins* **39,** 178–194
34. Nicholls, A., Bharadwaj, R., and Honig, B. (1993) *Biophys. J.* **64,** A166
35. Sayle, R. A., and Milner-White, E. J. (1995) *Trends Biochem. Sci.* **20,** 374
36. Roberts, J. R., Narasimhan, C., Hruz, P. W., Mitchell, G. A., and Miziorko, H. M. (1994) *J. Biol. Chem.* **269,** 17841–17846
37. Abascal, F., and Valencia, A. (2002) *Bioinformatics* **18,** 908–921
38. Yona, G., Linial, N., Tishby, N., and Linial, M. (1998) *Proc. Int. Conf. Intell. Syst. Mol. Biol.* **6,** 212–221
39. Rost, B., and Sander, C. (1993) *J. Mol. Biol.* **232,** 584–599
40. Rost, B., and Sander, C. (1994) *Proteins* **19,** 55–72
41. Mancia, F., Smith, G. A., and Evans, P. R. (1999) *Biochemistry* **38,** 7999–8005
42. Gertl, J. A. (2000) *Nat. Struct. Biol.* **7,** 171–173
43. Roberts, J. R., and Miziorko, H. M. (1997) *Biochemistry* **36,** 7594–7600
44. Miller, B. G., Hassell, A. M., Wolfenden, R., Milburn, M. V., and Short, S. A. (2000) *Proc. Natl. Acad. Sci. U. S. A.* **97,** 2011–2016
45. Holm, L., and Sander, C. (1997) *Proteins* **28,** 72–82
46. Abagyan, R. A., and Batalov, S. (1997) *J. Mol. Biol.* **273,** 355–368
47. Park, J., Teichmann, S. A., Hubbard, T., and Chothia, C. (1997) *J. Mol. Biol.* **273,** 349–354
48. Salamov, A. A., Suwa, M., Orengo, C. A., and Swindells, M. B. (1999) *Protein Eng.* **12,** 95–100
49. Chothia, C., and Lesk, A. M. (1986) *EMBO J.* **5,** 823–826
50. Holm, L., and Sander, C. (1996) *Science* **273,** 595–603